UC San Diego
UC San Diego Previously Published Works

Title

EEG microstates in early-to-middle childhood show associations with age, biological sex, and alpha power.

Permalink

https://escholarship.org/uc/item/5t97k13p

Journal

Human Brain Mapping, 44(18)

Authors

Hill, Aron
Bailey, Neil
Zomorrodi, Reza
et al.

Publication Date

2023-12-15

DOI

10.1002/hbm.26525

Copyright Information

Peer reviewed

RESEARCH ARTICLE

WILEY

EEG microstates in early-to-middle childhood show associations with age, biological sex, and alpha power

Aron T. Hill[1,2] | Neil W. Bailey[3,4] | Reza Zomorrodi[5] | Itay Hadas[6] |
Melissa Kirkovski[1,7] | Sushmit Das[8] | Jarrad A. G. Lum[1] | Peter G. Enticott[1,2]

[1]Cognitive Neuroscience Unit, School of Psychology, Deakin University, Geelong, Australia

[2]Department of Psychiatry, Central Clinical School, Monash University, Melbourne, Australia

[3]Monarch Research Institute, Monarch Mental Health Group, Sydney, Australia

[4]School of Medicine and Psychology, The Australian National University, Canberra, Australia

[5]Temerty Centre for Therapeutic Brain Intervention, Centre for Addiction and Mental Health, University of Toronto, Toronto, Canada

[6]Department of Psychiatry, School of Medicine, University of California San Diego, La Jolla, California, USA

[7]Institute for Health and Sport, Victoria University, Melbourne, Australia

[8]Azrieli Adult Neurodevelopmental Centre, Centre for Addiction and Mental Health, Toronto, Canada

Correspondence
Aron T. Hill, Cognitive Neuroscience Unit, School of Psychology, Deakin University, 221 Burwood Hwy, Burwood, Victoria, Australia.
Email: a.hill@deakin.edu.au

Abstract

Electroencephalographic (EEG) microstates can provide a unique window into the temporal dynamics of large-scale brain networks across brief (millisecond) timescales. Here, we analysed fundamental temporal features of microstates extracted from the broadband EEG signal in a large ($N = 139$) cohort of children spanning early-to-middle childhood (4–12 years of age). Linear regression models were used to examine if participants' age and biological sex could predict the temporal parameters *GEV*, *duration*, *coverage*, and *occurrence*, for five microstate classes (A–E) across both eyes-closed and eyes-open resting-state recordings. We further explored associations between these microstate parameters and posterior alpha power after removal of the $1/f$-like aperiodic signal. The microstates obtained from our neurodevelopmental EEG recordings broadly replicated the four canonical microstate classes (A to D) frequently reported in adults, with the addition of the more recently established microstate class E. Biological sex served as a significant predictor in the regression models for four of the five microstate classes (A, C, D, and E). In addition, *duration* and *occurrence* for microstate E were both found to be positively associated with age for the eyes-open recordings, while the temporal parameters of microstates C and E both exhibited associations with alpha band spectral power. Together, these findings highlight the influence of age and sex on large-scale functional brain networks during early-to-middle childhood, extending understanding of neural dynamics across this important period for brain development.

KEYWORDS
age, alpha power, biological sex, brain networks, EEG, microstates, neurodevelopment, neuroimaging

1 | INTRODUCTION

During early-to-middle childhood, the human brain undergoes extensive growth and reorganisation enabling the development of higher order cognitive functions, language, and social and emotional processes (Bunge & Wright, 2007; Chai et al., 2017; Gilmore et al., 2018; Long et al., 2017). Non-invasive functional neuroimaging of spontaneous (i.e., 'task free') neural activity patterns have enabled critical insight into brain dynamics across neurodevelopment. For example, resting-state functional magnetic resonance imaging (fMRI)

studies have revealed that as children develop, there is a shift in functional network architecture from locally focussed to more distributed patterns of neural communication (Fair et al., 2009; Long et al., 2017; Vogel et al., 2010). Further, longitudinal studies highlight increases in the strength of default mode network (DMN) connections throughout childhood and early adolescence (Fan et al., 2021; Sherman et al., 2014), which serve to facilitate maturation of complex neurocognitive abilities that are linked to both the DMN activity and connectivity strength (Hampson et al., 2006; Smallwood et al., 2021). However, the reliance of fMRI on the relatively slow (seconds) haemodynamic response limits its temporal precision precluding insight into more rapidly evolving alterations in brain dynamics. Further, the fMRI blood-oxygen-level-dependent (BOLD) signal provides only an indirect measure of neuronal activity and its exact relationship to underlying neurophysiology remains unclear (Ekstrom, 2010; Singh, 2012). Faster variations in neural activity, which are likely to provide additional complementary information on age-related changes in brain function can be assessed using electroencephalographic (EEG) recordings of electrical signals from neuronal ensembles (Buzsáki et al., 2012; Olejniczak, 2006). Despite lacking the spatial precision of fMRI, EEG benefits from extremely high (millisecond) temporal resolution, enabling analysis of highly transitory cortical activity, providing a powerful lens through which to examine functional network dynamics across neurodevelopment (Cohen, 2017; John et al., 1980; Uhlhaas et al., 2010). EEG is also silent, relatively inexpensive, easy to administer, and in the case of resting-state recordings, requires relatively little participant cooperation, thus making it very well suited to the collection of functional brain data in children.

EEG microstates provide a novel, and potentially powerful, avenue for examining spatio-temporal network dynamics across the lifespan. Microstates represent temporally discrete cortical activation patterns in the spatial dimension that remain quasi-stable for brief (∼60–120 ms) time periods before rapidly transitioning to a different spatial configuration of cortical activation (Lehmann et al., 1987; Michel & Koenig, 2018). Each distinct topographical pattern of cortical activity, or microstate 'class', represents a transient period of global network activity, with shifts between microstate classes over the millisecond time space of the EEG recording indicative of large-scale changes in functional brain organisation (Michel & Koenig, 2018; Zanesco et al., 2020). It has been shown that spontaneous EEG recorded at rest can be characterised by a relatively small number of microstates, typically four (labelled by previous research as canonical classes A, B, C, and D; see Figure 1), which can explain between ∼65% and 85% of the total topographic variance on the EEG record (Khanna et al., 2015; Michel & Koenig, 2018). The temporal features at these microstate classes demonstrate high test–retest reliability (Khanna et al., 2014), and appear to be relatively consistent across the adult lifespan (Khanna et al., 2015; Koenig et al., 2002), with more recent studies also beginning to establish additional classes beyond the canonical four (Das et al., 2022; Tarailis et al., 2023). The topographical features of several EEG-derived microstates have also been shown to overlap with well-defined fMRI-derived resting-state

networks (RSNs) (Britz et al., 2010; Custo et al., 2017; Musso et al., 2010).

Microstates are classically assessed in terms of their specific temporal parameters. These include the *global explained variance* (*GEV*), which reflects the percentage of total variance in the data explained by a given microstate class; average *duration* of time the microstate remains stable; the microstate's *coverage*, that is, the total amount of time it is present across the EEG recording; and its frequency of *occurrence* per second (Khanna et al., 2015; Lehmann et al., 1987). The use of these metrics to explore alterations in large-scale network activity
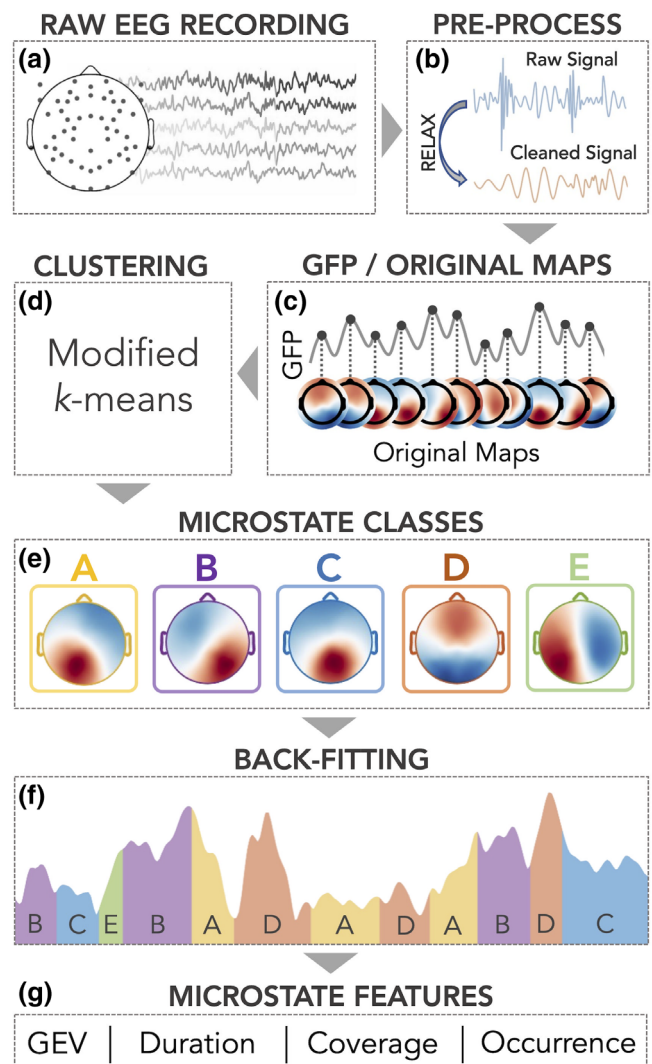
FIGURE 1 Graphical overview of the microstate analysis workflow. The spontaneous EEG recordings (a) were cleaned using the RELAX automated pre-processing pipeline (b). Data from sections of the EEG signal representing maximal global field potentials (GFP; c) were entered into the modified *k*-means clustering algorithm (d) to enable grouping into microstate classes based on topographic similarity (i.e., microstate prototypes; (e). Microstate prototypes were then back-fit to all of the EEG data (f). Finally, key microstate features (global explained variance, duration, coverage, and occurrence) were calculated (g).

during typical neurodevelopment, however, remains limited; to our knowledge, only four studies having specifically examined age-related changes in typically developing children (Bagdasarov et al., 2022; Koenig et al., 2002; Takarae et al., 2022; Tomescu et al., 2018). Initial work by Koenig et al. (2002) explored the four canonical (A-D) microstates extracted from spontaneous (eyes-closed) EEG recordings across individuals spanning a wide age-range (6–80 years). Participants were further broken into several putative developmental stages: childhood (defined as <12 years of age), early adolescence (12–16 years), late adolescence (>16 and <21 years), and adulthood (>21 years). The authors found a relatively undifferentiated pattern of microstate features across age in the childhood sample. However, qualitatively, average microstate durations did decline with increasing age, while each microstate's frequency of occurrence indicated a subtle upward trend. A later study by Tomescu et al. (2018), which also analysed eyes-closed spontaneous EEG across a wide age range (6–87 years), found that, overall, compared to females, males showed increased *occurrence* of microstate D and shorter *duration* of microstate C. Of note, females showed a relatively constant increase in the *duration* of microstate C from childhood into adulthood; while, despite showing increases in duration from childhood to adolescence (as well as during adulthood), the *duration* of microstate C showed a subtle reduction from adolescence to young adulthood in males. In contrast, microstates A and B were not found to differ between sexes.

In a study of eyes-open resting-state EEG comprising both typically developing and autistic children and adolescents (age-range: 7–19 years), Takarae et al. (2022) found a positive association between age and the *duration* of microstate C, which only reached significance in the typically developing sub-sample. As microstate temporal parameters have shown associations with the power of alpha oscillations (Croce et al., 2020; Milz et al., 2017), with these oscillations also demonstrating alterations in autism (Wang et al., 2013), Takarae et al. (2022) further explored potential links between EEG microstates extracted from the broadband EEG signal (0.5–40 Hz) and alpha power. These authors found a negative association between microstate C *duration* and alpha power and a positive association between microstate C *occurrence* and alpha power. These findings are the first, to our knowledge, to indicate a relationship between alpha oscillations, which represent the dominant cortical rhythm during relaxed wakefulness (Niedermeyer, 1999), and EEG microstates in children. This extends research in adults that has indicated an association between the temporal parameters of various microstate classes and alpha power (Croce et al., 2020; Milz et al., 2017). However, as these authors analysed the entire EEG signal, which is known to contain a mix of both neuronal oscillations and broadband aperiodic (i.e., $1/f$-like non-oscillatory) activity (Donoghue, Haller, et al., 2020; He, 2014) it is likely that their measures of spectral power actually captured both periodic and aperiodic activity (Donoghue et al., 2021; Donoghue, Haller, et al., 2020; He, 2014). Work is therefore needed to assess this potential association after first disentangling the periodic and aperiodic signal to ensure power values capture true oscillatory activity. Finally, recent work by Bagdasarov et al. (2022) using eyes-closed resting-state EEG in 4–8-year-old children found associations

between microstates C and D and children's' age and biological sex. Specifically, microstate C *duration* was greater in males compared to females. Additionally, *GEV*, *coverage* and *occurrence* for microstate D all decreased with increasing age in males, but not females; while *duration* decreased with age in males, while increasing for females.

Building on these past observations, the primary aim of this study was to extend research investigating EEG microstates during neurodevelopment by conducting a comprehensive analysis of spontaneous EEG activity captured across a large sample of children spanning early-to-middle childhood. To achieve this, we analysed both eyes-closed and eyes-open resting-state EEG recordings from 139 children ranging from 4 to 12 years of age. Differences in microstate temporal parameters were explored separately for both recordings, thus enabling us to investigate resting-state dynamics across these two perceptual states, which are known to induce changes in neural oscillations and brain network activity (Agcaoglu et al., 2019; Li, 2010). We further assessed associations between these features and participants' age and biological sex. Finally, we also explored associations between microstate parameters and alpha power after first removing the aperiodic signal through spectral parameterisation (Donoghue, Haller, et al., 2020). As this was an exploratory study, we did not have specific directional hypotheses. However, we broadly predicted that microstate features would: (i) show changes across the 4–12 year age range, (ii) differ between sexes, and (iii) show an association with aperiodic-adjusted alpha power.

2 | METHODS

2.1 | Participants

The sample comprised 139 English speaking children (67 female; average age = 9.41 years, SD = 1.95; age range: 4–12 years [female: 9.11 years; SD = 1.96; male: 9.69 years; SD = 1.91]). Participants were described as being typically developing by their primary caregiver, with no child in the dataset having been diagnosed with any neurological, psychiatric, or genetic disorder. Ethical approval was provided by the Deakin University Human Research Ethics Committee (2017–065), and approval to approach public schools was granted by the Victorian Department of Education and Training (2017_003429).

2.2 | Procedure

EEG data were collected during a single recording session for each child at Deakin University, or in a quiet room at the participants' school. Written consent was obtained from the parent or legal guardian of each child prior to the study commencing. Key details of the experimental protocol were also verbally explained to each child who then agreed to participate. Data reported in this study were collected as part of a larger investigation into the development of the social brain in childhood (for further information see Bigelow et al., 2022; Hill et al., 2022).

2.3 | EEG acquisition

EEG data were recorded at rest via a 64-channel HydroCel Geodesic Sensor Net (Electrical Geodesics, Inc., USA) containing Ag/AgCl electrodes surrounded by electrolyte-wetted sponges. Data were recorded in a dimly lit room using NetStation software (version 5.0) via a Net Amps 400 amplifier using a sampling rate of 1 KHz, with an online reference at electrode Cz. Electrode impedances were checked to ensure they were < 50 KOhms prior to recordings commencing. EEG was recorded for 2 min with eyes-open (participants seated with their gaze directed at a fixation cross on a computer monitor), and 2 min while participants had their eyes-closed.

2.4 | EEG pre-processing

Data were pre-processed in MATLAB (R2020a; The Mathworks, Massachusetts, USA) using the EEGLAB toolbox (Delorme & Makeig, 2004) and custom scripts. The Reduction of Electroencephalographic Artifacts (RELAX) software (Bailey, Biabani, et al., 2023; Bailey, Hill, et al., 2023) was used to clean each EEG file. This automated pipeline uses empirical approaches to identify and reduce artefacts within the data, including the use of both multi-channel Wiener filters and wavelet enhanced independent component analysis (ICA). Briefly, data were bandpass filtered (0.5–80 Hz) using a fourth-order Butterworth filter with zero-phase. Data were then notch filtered (47–53 Hz) to remove line noise, and any bad channels were removed using a multi-step process incorporating the 'findNoisyChannels' function from the PREP pipeline (Bigdely-Shamlo et al., 2015). Multi-channel Wiener filtering (Somers et al., 2018) was used to initially clean blinks, muscle activity, horizontal eye movement and drift, followed by robust average re-referencing (Bigdely-Shamlo et al., 2015), and wavelet-enhanced ICA (Castellanos & Makarov, 2006), with components for cleaning identified using the automated independent component (IC) classifier IClabel (Pion-Tonachini et al., 2019). As a final step, all pre-processed data files were also visually inspected to further assess recording quality and check for any electrographic signs of excessive somnolence. Additional details on the data pre-processing procedure can be found in Hill et al. (2022).

2.5 | Microstate analysis

Prior to running the microstate analyses, the EEG data were bandpass filtered between 1 and 40 Hz (fourth order zero-phase Butterworth filter) and were down-sampled to 250 Hz to reduce computational burden (Bochet et al., 2021). Microstate analysis was conducted in MATLAB implementing the open-source Microstate EEGLAB toolbox (version 1.0) (Poulsen et al., 2018). First, the global field power (GFP), which represents the standard deviation of the EEG signal across all electrodes (Lehmann & Skrandies, 1980), was calculated for each participant from the spontaneous EEG recordings. Datapoints corresponding to GFP maxima (i.e., maps containing high signal-to-noise ratio) were then entered into the modified k-means clustering algorithm (Koenig et al., 2002; Pascual-Marqui et al., 1995), which was used to find from 3-to-8 microstate prototypes. The modified k-means method is polarity invariant meaning that no distinction is made between proportional, but opposite, topographical maps when assigning microstate clusters (Pascual-Marqui et al., 1995). The cluster analysis was set to undergo 50 random initialisations with the maximum number of iterations set to 1000. 1000 GFP peaks per subject entered the segmentation, with the minimum distance between peaks set to 10 ms, as advised by Poulsen et al. (2018). Based on visual inspection of the topographies and measures of fit (global explained variance [GEV] and cross-validation [CV] criterion) (Poulsen et al., 2018), for the EEG clustered with between 3-and-8 microstates, we identified five prototypical microstate maps (A to E) that adequately described the data for both the eyes-closed and eyes-open recordings (Figure 2; see Figure S1 for plots of GEV and CV values for the data). This also represented a pragmatic compromise between the requirement for both specificity and generalisability, the former typically benefitting from an increasing number of microstates, and the latter benefitting from a relatively low number of microstates (Michel & Koenig, 2018). These microstate classes were then back-fitted to each participant's EEG data. As spontaneous EEG recordings frequently contain unwanted noise, which can contribute to short microstate segments that emerge after clustering or backfitting of the data (Musaeus et al., 2019; Poulsen et al., 2018), we applied the default 'small segment rejection' temporal smoothing approach from the Microstate EEGLAB Toolbox (Poulsen et al., 2018) to redistribute segments <30 ms to the next best fitting microstate. Finally, the temporal parameters GEV, duration, coverage, and occurrence were calculated for each microstate class (see Figure 1 for microstate analysis overview).

2.6 | Calculation of alpha power

Alpha power was calculated to enable exploration of its potential association with microstate temporal parameters. The EEG data were first converted to the frequency domain using the Welch power spectral density (PSD) method in MATLAB (2-second Hamming window with 50% overlap). In order to obtain alpha power values for each participant we used a spectral parameterisation approach implemented via the Fitting Oscillations and One Over f (FOOOF) toolbox (version 1.0.0; https://fooof-tools.github.io/fooof/) (Donoghue, Haller, et al., 2020). This model-driven approach has the benefit of obtaining alpha peaks within the EEG spectra in terms of their specific centre frequency for each individual, while also controlling for the aperiodic (i.e., non-oscillatory) broadband signal (Donoghue, Haller, et al., 2020; Ostlund et al., 2022). Algorithm settings were set as: peak width limits = [1,12]; maximum number of peaks = 8; minimum peak height = 0.0; peak threshold = 2; and aperiodic mode = fixed. Power spectra were parameterised across the frequency range 1 to 40 Hz
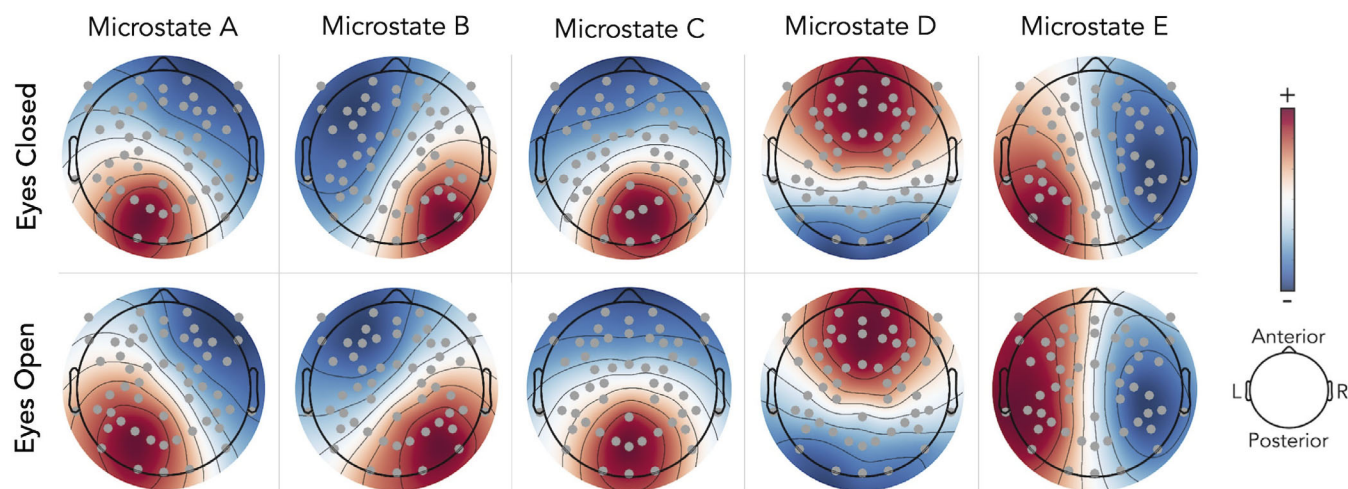
FIGURE 2 Topographic plots of the five EEG microstate classes (a–e) for the eyes-closed and eyes-open conditions. These closely resembled the orientations previously reported in adults, specifically, Microstate A: right anterior to left posterior; Microstate B: left anterior to right posterior; Microstate C: frontal to occipital; Microstate D: medial anterior to occipital; Microstate E: left to right. Microstates were derived using a polarity invariant (modified *K*-means) clustering algorithm.

(for power spectra plots see Figures S2 and S3). Alpha power was then extracted from the midline parieto-occipital electrode (POz) for the peak within the 7–13 Hz range. This electrode was selected based on its posterior location where alpha power is often maximal (Klimesch et al., 2005), with the majority (>94%) of participants demonstrating a detectable alpha peak in this region over-and-above the aperiodic signal.

2.7 | Statistical analysis

Statistical analyses were conducted using R (R Core Team, 2020). Prior to running the analyses, the data were screened for outliers and any extreme values (larger/smaller than 1.5*IQR above or below the upper and lower interquartile ranges, respectively) were removed. Power analysis indicated that our sample size was well powered ($1 - \beta = 0.92$) to detect a regression slope using a multiple linear regression with two predictors with a small-to-moderate effect size ($f^2 = 0.1$) and $\alpha = 0.05$ (Faul et al., 2007). Multiple linear regression models were used to assess the ability for age and sex to predict *GEV*, *duration*, *coverage*, or *occurrence* for each of the five microstate classes. Analyses were run separately for the eyes-closed and eyes-open EEG data. Multiple comparison corrections were applied to the overall regression models using the Bonferroni–Holm method (Holm, 1979) to account for the five microstates classes examined. Individual predictors (i.e., age and sex) were only examined if the overall model showed significance after correction and were further corrected to account for the four microstate parameters (corrected alpha = 0.0125). Associations between microstate parameters and alpha power were explored using non-parametric (Spearman) correlations. These were run separately for each temporal parameter for each of the five microstates for both the eyes-

closed and eyes-open conditions (Bonferroni corrected). Additional one-way repeated measures ANOVAs were also run to compare differences in *GEV*, *duration*, *coverage*, and *occurrence* between the five microstate classes for the eyes-closed and eyes-open data with post-hoc analyses of simple main effects performed using pairwise comparisons (Bonferroni corrected) and are reported in the Data S1. Finally, we also computed Pearson's spatial correlations for each of the five microstate classes between the eyes-closed and eyes-open recordings to assess for topographic similarity between the two conditions.

3 | RESULTS

Four of the microstate maps obtained for both the eyes-closed and eyes-open conditions strongly resembled the canonical microstates A, B, C, and D previously reported in the literature (Khanna et al., 2015; Michel & Koenig, 2018; Tarailis et al., 2023), while the fifth map resembled the more recently described microstate E (Custo et al., 2017; Das et al., 2022; Ke et al., 2021) (sometimes also referred to as microstate F (Tarailis et al., 2023); Figure 2; scalp field potential data pertaining to each microstate template map is also provided in Table S2). Together, the five microstates explained 69.2% (eyes-closed) and 68.4% (eyes-open) of the total global variance, which is broadly in line with previous reports (Custo et al., 2017; Michel & Koenig, 2018) (plots indicating GEV and cross validation criterion [CV] values for microstate clusters are provided in Figure S2). No differences in age were apparent between male and female participants ($t(135.63) = 1.77$, $p = 0.080$). Figure 3 provides an overview of participants' age and sex via density plots and Figure 4 provides an overview of the temporal parameters for each microstate separately for the eyes-closed and eyes-open recordings. Descriptive statistics of

the temporal features for each of the five microstate classes are provided in Table 1. Spatial correlations indicated that the microstate maps extracted from the eyes-closed and eyes-open recordings showed relatively strong similarity, overall ($r = 0.83$, 0.88, 0.92, 0.93, 0.71 for maps A to E, respectively; Figure 5). We further ran spatial correlations between microstate maps run after also extracting microstates for males and females separately on both the eyes-closed and eyes-open recordings. These results are provided in Figure S4.
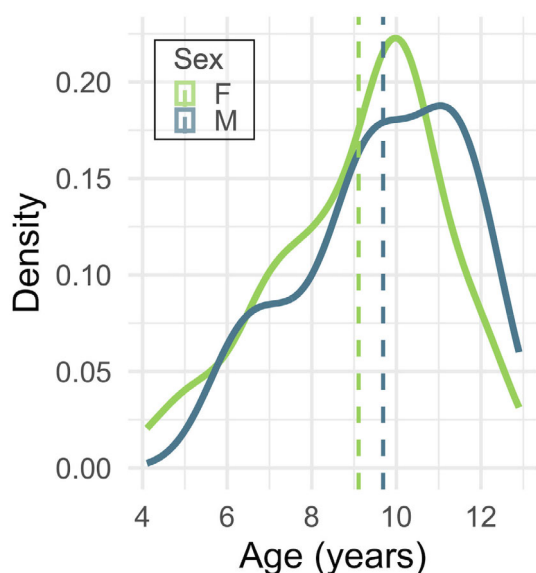
FIGURE 3 Density plot showing the age distribution for both females and males. Dashed vertical lines indicate mean age for each group. Age did not significantly differ between the two sexes ($p > .05$).

## 3.1 | Age and sex effects on microstate parameters

Multiple linear regression models with participants' age and sex as predictor variables, and microstate parameter (either *GEV*, *duration*, *coverage*, or *occurrence*) as the outcome variable were run separately for the eyes-closed and eyes-open conditions. Results are summarised in Table 2, with key findings also highlighted below.

3.1.1 | Microstate A

For the eyes-closed data, the overall regression model was significant for all four microstate parameters (*GEV*, *duration*, *coverage*, and *occurrence*). In each instance, of the two predictors, only sex was found to significantly contribute to the model. Specifically, on average, females had a higher *GEV* ($t(131) = -4.871$, $p < 0.001$), *duration* ($t(131) = -3.684$, $p < 0.001$), *coverage* ($t(131) = -4.978$, $p < 0.001$), and *occurrence* ($t(134) = -5.271$, $p < 0.001$) than males. For the eyes-open data, the overall model was significant for all four microstate parameters. As with the eyes-closed data, only sex significantly contributed to the model. On average, females had higher *GEV*, ($t(126) = -5.314$, $p < 0.001$), *duration*, ($t(127) = -4.125$, $p < 0.001$), *coverage*, ($t(128) = -5.035$, $p < 0.001$), and *occurrence*, ($t(134) = -5.846$, $p < 0.001$), than males.
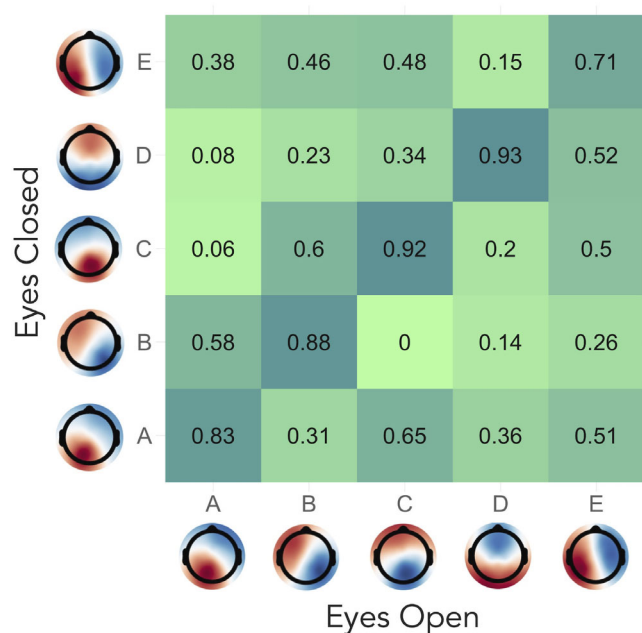
3.1.2 | Microstate B

For the eyes-closed recordings, the overall regression model was not significant for any of the microstate parameters. For the eyes-open
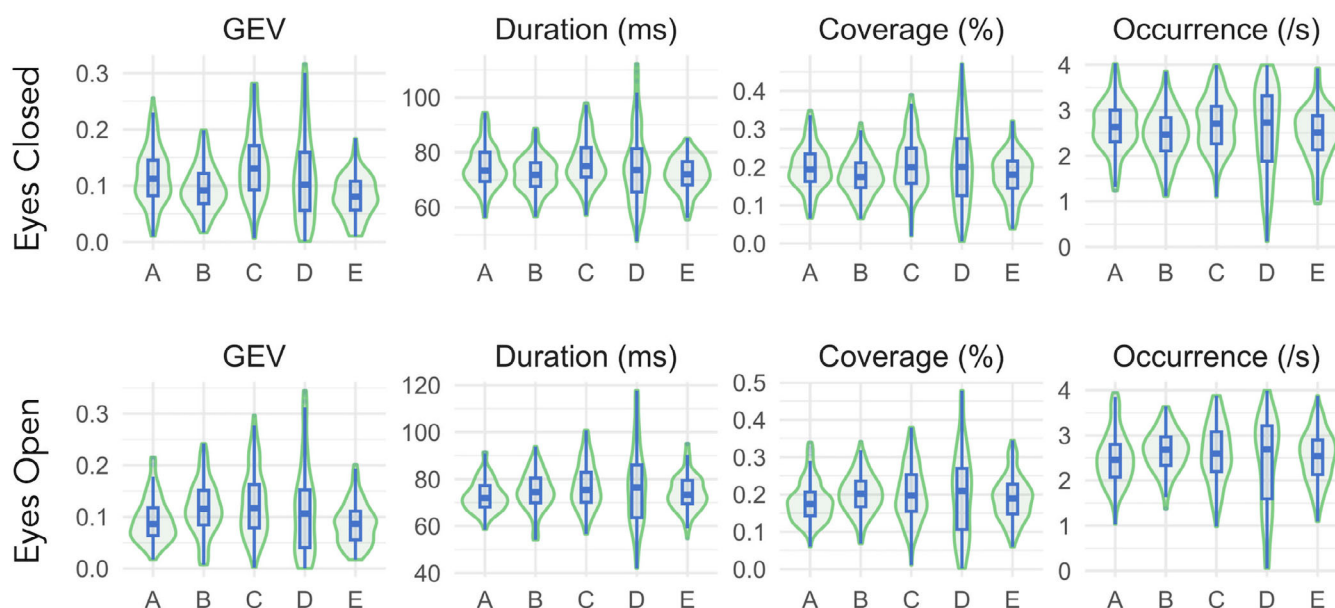
FIGURE 4 Violin plots showing the values for *GEV*, *duration*, *coverage*, and *occurrence* for each of the five microstate classes (A–E) separately for the eyes-closed and eyes-open recordings.

TABLE 1 Microstate descriptive statistics.

Measure	Microstate A	Microstate B	Microstate C	Microstate D	Microstate E
GEV					
Eyes-closed mean (SD)	0.13 (0.07)	0.10 (0.05)	0.14 (0.07)	0.13 (0.10)	0.09 (0.05)
Eyes-open mean (SD)	0.11 (0.08)	0.12 (0.06)	0.13 (0.08)	0.13 (0.10)	0.10 (0.06)
Duration (ms)					
Eyes-closed mean (SD)	76.66 (13.89)	73.18 (8.27)	77.24 (10.55)	77.54 (17.72)	73.50 (9.68)
Eyes-open mean (SD)	75.75 (13.27)	74.95 (8.77)	78.15 (12.15)	78.00 (17.94)	76.45 (16.95)
Coverage (%)					
Eyes-closed mean (SD)	0.21 (0.08)	0.19 (0.06)	0.21 (0.07)	0.21 (0.12)	0.19 (0.07)
Eyes-open mean (SD)	0.20 (0.09)	0.19 (0.07)	0.21 (0.08)	0.20 (0.12)	0.20 (0.08)
Occurrence (/s)					
Eyes-closed mean (SD)	2.62 (0.59)	2.48 (0.57)	2.68 (0.63)	2.54 (0.95)	2.46 (0.67)
Eyes-open mean (SD)	2.52 (0.61)	2.52 (0.66)	2.58 (0.70)	2.38 (1.01)	2.53 (0.58)

FIGURE 5 Spatial correlations (absolute correlation coefficient) between the eyes-closed and eyes-open microstate topographies. Note, as the polarity invariant modified k-means clustering algorithm was used, microstate polarity can be ignored.

recordings, the model reached significance only for *occurrence*; however, neither age ($t(125) = -1.370$, $p = 0.173$), nor sex ($t(125) = -1.842$, $p = 0.068$), significantly contributed to the model.

3.1.3 | Microstate C

For microstate C, the overall model did not reach significance for any microstate parameter for the eyes-closed dataset. However, for the eyes-open recordings, the model was significant for *GEV*, *coverage*,

and *occurrence*. On average, females had higher *GEV* ($t(131) = -4.248$, $p < 0.001$), *coverage* ($t(133) = -3.090$, $p = 0.002$), and *occurrence* ($t(134) = -2.960$, $p = 0.004$) than males. Age did not contribute to the model for any parameter.

3.1.4 | Microstate D

For microstate D, the overall model was significant for all four microstate parameters for the eyes-closed condition, and in all instances, sex was found to be the only significant contributor to the model. Specifically, on average, males had higher *GEV* ($t(130) = 9.247$, $p < 0.001$), *duration* ($t(130) = 8.701$, $p < 0.001$), *coverage* ($t(133) = 9.162$, $p < 0.001$), and *occurrence* ($t(136) = 10.254$, $p < 0.001$) than females. For the eyes-open data, the overall model was also significant for all parameters. On average, males had higher *GEV* ($t(130) = 8.348$, $p < 0.001$), *duration* ($t(134) = 9.427$, $p < 0.001$), *coverage* ($t(135) = 10.995$, $p < 0.001$), and *occurrence* ($t(136) = 11.700$, $p < 0.001$) than females.
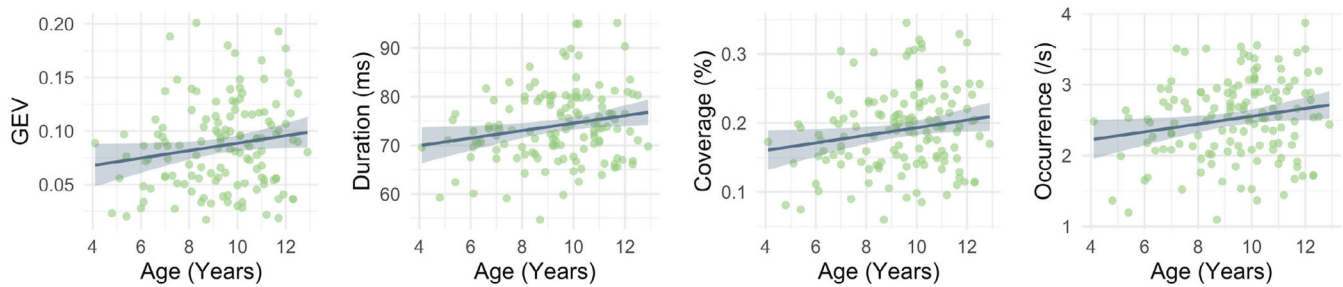
3.1.5 | Microstate E

For the eyes-closed data, the overall regression model was significant for all four microstate parameters. Only sex significantly contributed to the model. On average, females had a higher *GEV* ($t(130) = -3.574$, $p < 0.001$), *duration* ($t(129) = -2.921$, $p = 0.004$), *coverage* ($t(131) = -3.312$, $p = 0.001$), and *occurrence* ($t(131) = -3.605$, $p < 0.001$) than males. For the eyes-open data, both age and sex contributed. For *GEV*, only sex contributed to the model ($t(130) = -2.979$, $p = 0.003$), with females having higher values than males. For *duration*, age was the only significant contributor ($t(130) = 2.600$, $p = 0.010$). For *coverage*, neither predictor significantly contributed after multiple comparison correction, with age falling just above the Bonferroni corrected alpha ($p = 0.0152$ [Bonferroni alpha = 0.0125]).

TABLE 2 Multiple linear regression analyses examining the effects of participants' age and sex on the four microstate parameters.

	GEV	Duration	Coverage	Occurrence
Microstate A				
Eyes closed	$F(2,131) = 12.37, R^2 = 0.159,$ $p < 0.001$	$F(2,131) = 7.109, R^2 = 0.098,$ $p = 0.005$	$F(2,131) = 12.690,$ $R^2 = 0.162, p < 0.000$	$F(2,134) = 14.210,$ $R^2 = 0.175, p < 0.001$
Age	−0.000 (0.002)	−0.053 (0.332)	0.000 (0.002)	−0.000 (0.023)
Sex	−0.039 (0.008)**	−4.775 (1.296)**	−0.047 (0.009)**	−0.466 (0.088)**
Eyes Open	$F(2,126) = 14.35, R^2 = 0.186,$ $p < 0.001$	$F(2,127) = 8.595, R^2 = 0.119,$ $p = 0.001$	$F(2,128) = 12.700,$ $R^2 = 0.166, p < 0.000$	$F(2,134) = 17.090,$ $R^2 = 0.203, p < 0.001$
Age	0.003 (0.002)	0.056 (0.281)	0.002 (0.002)	0.0218 (0.023)
Sex	−0.037 (0.007)**	−4.597 (1.114)**	−0.045 (0.009)**	−0.534 (0.091)**
Microstate B				
Eyes closed	$F(2,131) = 3.261, R^2 = 0.047,$ $p = 0.078$	$F(2,130) = 2.305, R^2 = 0.034,$ $p = 0.208$	$F(2,131) = 3.148, R^2 = 0.046,$ $p = 0.092$	$F(2,135) = 2.482, R^2 = 0.035,$ $p = 0.175$
Age	−0.004 (0.002)	−0.577 (0.279)	−0.005 (0.002)	−0.053 (0.024)
Sex	−0.006 (0.007)	−0.305 (1.101)	−0.001 (0.009)	−0.012 (0.095)
Eyes open	$F(2,133) = 0.771, R^2 = 0.011,$ $p = 0.465$	$F(2,135) = 1.049, R^2 = 0.015,$ $p = 0.353$	$F(2,127) = 1.655, R^2 = 0.025,$ $p = 0.195$	$F(2,125) = 3.137, R^2 = 0.048,$ $p = 0.047$
Age	−0.003 (0.002)	−0.446 (0.362)	−0.003 (0.002)	−0.028 (0.020)
Sex	−0.003 (0.009)	1.333 (1.413)	−0.012 (0.009)	−0.150 (0.091)
Microstate C				
Eyes closed	$F(2,134) = 3.323, R^2 = 0.047,$ $p = 0.078$	$F(2,132) = 1.524, R^2 = 0.023,$ $p = 0.222$	$F(2,135) = 1.523, R^2 = 0.022,$ $p = 0.222$	$F(2,134) = 1.108, R^2 = 0.016,$ $p = 0.333$
Age	0.000 (0.003)	0.019 (0.380)	0.000 (0.003)	0.011 (0.026)
Sex	−0.027 (0.011)	−2.560 (1.473)	−0.021 (0.012)	−0.147 (0.1000)
Eyes open	$F(2,131) = 9.288, R^2 = 0.124,$ $p = 0.001$	$F(2,133) = 3.692, R^2 = 0.053,$ $p = 0.055$	$F(2,133) = 4.806, R^2 = 0.067,$ $p = 0.029$	$F(2,134) = 4.397, R^2 = 0.062,$ $p = 0.039$
Age	−0.000 (0.003)	−0.037 (0.427)	0.001 (0.003)	0.007 (0.028)
Sex	−0.045 (0.011)**	−4.458 (1.666)*	−0.0393 (0.0127)*	−0.326 (0.110)*
Microstate D				
Eyes closed	$F(2,130) = 43.030,$ $R^2 = 0.398, p < 0.001$	$F(2,130) = 37.900,$ $R^2 = 0.368, p < 0.001$	$F(2,133) = 42.25, R^2 = 0.389,$ $p < 0.001$	$F(2,136) = 53.38, R^2 = 0.440,$ $p < 0.001$
Age	−0.001 (0.003)	−0.371 (0.489)	−0.002 (0.004)	−0.009 (0.032)
Sex	0.099 (0.011)**	16.547 (1.902)**	0.132 (0.014)**	1.260 (0.123)**
Eyes open	$F(2,130) = 34.86, R^2 = 0.349,$ $p < 0.001$	$F(2,134) = 44.460,$ $R^2 = 0.399, p < 0.001$	$F(2,135) = 60.480,$ $R^2 = 0.473, p < 0.001$	$F(2,136) = 68.46, R^2 = 0.502,$ $p < 0.001$
Age	−0.004 (0.003)	−0.993 (0.577)	−0.006 (0.004)	−0.053 (0.032)
Sex	0.103 (0.012)**	21.022 (2.230)**	0.157 (0.0143)**	1.447 (0.124)**
Microstate E				
Eyes closed	$F(2,130) = 6.843, R^2 = 0.095,$ $p = 0.003$	$F(2,129) = 5.502, R^2 = 0.079,$ $p = 0.015$	$F(2,131) = 5.738, R^2 = 0.081,$ $p = 0.020$	$F(2,131) = 6.611, R^2 = 0.092,$ $p = 0.006$
Age	−0.001 (0.002)	−0.288 (0.273)	−0.000 (0.002)	0.001 (0.026)
Sex	−0.022 (0.006)**	−3.132 (1.072)*	−0.032 (0.010)*	−0.367 (0.102)**
Eyes open	$F(2,130) = 6.431, R^2 = 0.090,$ $p = 0.004$	$F(2,130) = 4.426, R^2 = 0.064,$ $p = 0.041$	$F(2,132) = 4.826, R^2 = 0.068,$ $p = 0.029$	$F(2,135) = 4.465, R^2 = 0.062,$ $p = 0.039$
Age	0.004 (0.002)	0.854 (0.329)*	0.006 (0.003)	0.062 (0.025)*
Sex	−0.021 (0.007)*	−2.302 (1.277)	−0.022 (0.010)	−0.185 (0.095)

Note: For the overall regression model, alpha values shown are after Bonferroni–Holm multiple comparison corrections for the five microstate classes (A–E). Values for age and sex are the coefficient estimate, with standard error in parentheses and stars denoting significance after multiple comparison correction (*$p < .01$, **$p < .000$).

FIGURE 6 Scatterplots showing the association between age and *GEV*, *duration*, *coverage*, and *occurrence* for microstate E (eyes-open recordings). Of the four parameters, age significantly contributed to the regression model only for *duration* and *occurrence* after multiple comparison correction.

Finally, for *occurrence*, age was the only significant predictor ($t(135)$ = 2.552, p = 0.012). Scatterplots depicting the positive associations between age and each of the temporal parameters for microstate E are shown in Figure 6.

3.2 | Associations with alpha power

Significant associations were observed between aperiodic-adjusted alpha power and microstates C and E. Specifically, for the eyes-closed data, significant positive correlations were obtained between alpha power and microstate C *GEV* (rho = 0.264, p = 0.002), *duration* (rho = 0.225, p = 0.009), *coverage* (rho = 0.280, p < 0.001), and *occurrence* (rho = 0.276, p = 0.001). Conversely, significant negative associations were observed between microstate E and alpha power for *GEV* (rho = −0.257, p = 0.003), *coverage* (rho = −0.264, p = 0.002), and *occurrence* (rho = −0.300, p < 0.001). For the eyes-open recordings, significant correlations were present across all four parameters for microstate C: *GEV* (rho = 0.258, p = 0.004), *duration* (rho = 0.239, p = 0.007), *coverage* (rho = 0.360, p < 0.001), and *occurrence* (rho = 0.382, p < 0.001). No other significant correlations were observed. Associations between alpha power and temporal parameters for each microstate are additionally provided in Table S1, with scatterplots showing key associations shown graphically in Figure 7.

4 | DISCUSSION

We have presented evidence that EEG-derived microstates recorded across early-to-middle childhood demonstrate similar topographies to those observed in adults, while regression models also indicated that participants' age and biological sex could predict several specific microstate temporal features. Finally, we further found associations between aperiodic-adjusted alpha power and microstates C and E. Brain network architecture is known to change substantially across the lifespan (Betzel et al., 2014; Chai et al., 2017). This is particularly apparent during neurodevelopment, where RSNs demonstrate considerable reorganisation and functional segregation (Gu et al., 2015;

Power et al., 2010). It is therefore likely that the spatio-temporal properties of large-scale cortical network activity, as reflected by microstates, might also change throughout early-to-middle childhood in line with known structural and functional network alterations that occur during neurodevelopment (Casey et al., 2005; Huang et al., 2015). We found that both the eyes-closed and eyes-open EEG recordings yielded microstate topographies in this cohort of children resembling the canonical microstate classes A to D frequently reported in adults (Khanna et al., 2015; Michel & Koenig, 2018; Tarailis et al., 2023), with the addition of the more recently described microstate E (e.g., Baldini et al., 2023; Brechet et al., 2019; Custo et al., 2017; Das et al., 2022). These observations corroborate similar recent findings from eyes-closed resting-state recordings in children spanning a similar developmental period (4–8 years) (Bagdasarov et al., 2022), while also further extending this finding to spontaneous eyes-open EEG data. This lends support to the relative stability of broad microstate topographies across age, despite observations of age-related alterations to specific microstate temporal features such as *duration*, *coverage*, and *occurrence*. Age-related changes in specific temporal parameters of microstates have been previously reported elsewhere (Koenig et al., 2002; Tomescu et al., 2018) and have also been shown be altered across several neurodevelopmental, psychiatric, and neurological illnesses (Andreou et al., 2014; Baldini et al., 2023; Bochet et al., 2021; da Cruz et al., 2020), thus highlighting their clinical relevance. More broadly, these findings appear to parallel previous fMRI work characterising functional brain organisation and development in children spanning a similar ages (e.g., 7–9 years; Supekar et al., 2009).

4.1 | Age effects on microstate features

Out of the five microstates, only microstate E showed significant associations with age in the present cohort, with these associations only apparent in the eyes-open condition. Specifically, while all four of the microstate parameters (*GEV*, *duration*, *coverage*, *occurrence*) were seen to increase as a function of age (Figure 6), age was only found to significantly contribute to the model for *duration* and *occurrence* after multiple comparison corrections were applied. We also note that, while we refer here to the topography with left-to-right configuration
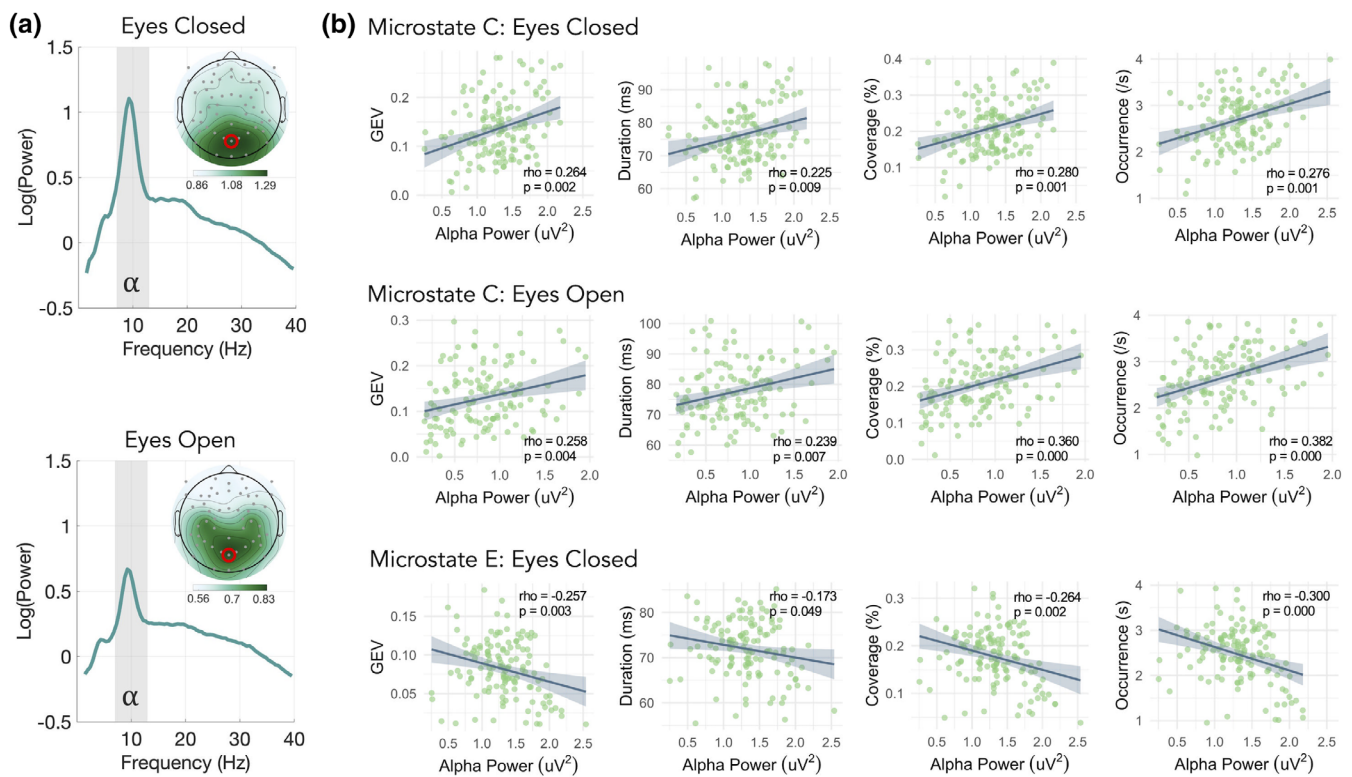
FIGURE 7 Associations between EEG alpha power and temporal parameters for microstates C and E. (a) Plots of the aperiodic-adjusted EEG spectra taken from the posterior (POz; red circle) electrode with topographic plots showing the overall scalp distribution of alpha power. (b) Correlations between alpha power and microstates C (eyes-closed, eyes-open) and microstate E (eyes closed). Alpha power was significantly positively associated with all four microstate features (*GEV, duration, coverage, occurrence*) for microstate C in the eyes-closed and eyes-open recordings. Significant negative associations were also observed for alpha power and microstate E *GEV, coverage,* and *occurrence* in the eyes-closed condition.

as microstate E, in line with other studies (e.g., Baldini et al., 2023; Brechet et al., 2019; Custo et al., 2017; Das et al., 2022; D'Croz-Baron et al., 2019; Ke et al., 2021; Takarae et al., 2022; Tarailis et al., 2021), inconsistent microstate labelling across studies has also seen this microstate labelled as microstate F (see Tarailis et al. (2023) for a recent in-depth review of resting-state EEG microstates). As microstate E is relatively newly described, only limited information presently exists on its functional relevance (Tarailis et al., 2023). However, using an approach that enabled source localisation of the microstate topographies, Custo et al. (2017) were able to establish that microstate E demonstrated activity associated with key regions of the DMN, such as the anterior cingulate cortex (ACC), posterior cingulate cortex (PCC), and precuneus; while Brechet et al. (2019) found the strongest activity for microstate E in the medial prefrontal cortex, which also represents a key cortical area of the DMN (Raichle, 2015). While still speculative at this stage, it is possible that the age-related increases in these temporal parameters observed in the present study might reflect maturational changes in regions of the DMN related to spontaneous cognition, theory of mind, and self-referential processing (Buckner et al., 2008; Padmanabhan et al., 2017; Tarailis et al., 2023). However, why these specific associations were not also reflected in the eyes-closed condition remains uncertain. Future studies aimed at directly examining possible links between microstate E parameters

and DMN-salient cognitive processes in developmental cohorts could be useful for investigating this in more detail.

Consistent with past research, our results also indicate that age-related changes in microstate features are dependent on the specific microstate class (Koenig et al., 2002). The tendency for an increase in *occurrence* with increasing age differs from findings by Tomescu et al. (2018) who reported a tendency for reduced microstate *occurrence* with increasing age; although, microstate D showed a reverse effect (i.e., occurrence increased with age). However, it is important to note that these authors only analysed eyes-closed EEG recordings, included participants spanning a much wider age range (6–87 years), and only investigated the four canonical microstates A-D. These methodological differences might have potentially contributed to these differing observations. In particular, the inclusion of adult and elderly participants by Tomescu et al. (2018) might have reduced the potential to detect associations specific to the childhood age group, which was the focus of our present study. Indeed, we also did not find any associations between age and any of the microstate parameters in the eyes-closed condition. A more recent study by Bagdasarov et al. (2022), which explored spontaneous microstate dynamics in participants of similar age to our present cohort (4–8 years) using eyes-closed recordings, did report relationships between parameters of microstates C and D and age and sex; however, their study also only

extracted the four canonical microstates (A–D), thus prohibiting direct comparisons with our findings for microstate E. Future studies in developmental cohorts using a broader range of microstates is therefore warranted to further investigate associations with age.

4.2 | Sex effects on microstate features

Overall, our results indicate strong associations between microstate parameters and biological sex, with four of the five microstate classes (A, C, D, and E) having at least one feature that was predicted by sex. For microstates A, C, and E, there was an overall tendency for females to demonstrate higher values for the various microstate parameters. This was most apparent for microstate A, where females scored higher than males for all parameters across both the eyes-closed and eyes-open conditions, but similar patterns were also frequently seen for microstates C and E. In contrast, males tended to show higher values than females for microstate D (see Table 2; scatterplots comparing each of the microstate parameters against age are also provided Figure S6).

To our knowledge, only two previous studies have investigated sex-related differences in microstate parameters in developmental cohorts, both of which used eyes-closed EEG recordings only. In opposition to our findings, Bagdasarov et al. (2022) found longer durations of microstate C in males compared to females in a cohort of children ages between 4 and 8 years. However, in contrast, Tomescu et al. (2018) reported shorter microstate C durations in males compared to females, but this study comprised individuals across a broad age-range (6–87 years). Our present finding of longer *duration* in females for microstate C therefore most strongly aligns with Tomescu et al. (2018) who also reported more prolonged durations of this microstate class in females. However, a noteworthy difference is that we observed this only in the eyes-open recordings. In addition, our results further extended this observation to *GEV, coverage, and occurrence*. Similarly, our finding of higher *occurrence* of microstate D in males also aligns Tomescu et al., who reported microstate D to occur more frequently in males than females. However, as with microstate C, differences in the present study also extended to other microstate parameters. Although the precise functional significance of microstate C remains uncertain (Tarailis et al., 2023), there is some evidence to suggest a relationship with brain regions forming part of the DMN, a task-negative system well characterised in fMRI literature (Custo et al., 2017; Seitzman et al., 2017; Tarailis et al., 2023). For instance, source localisation of microstate C highlights cortical generators in the PCC and precuneus that belong to the DMN (Custo et al., 2017). This might suggest that females tend to spend more time in states related to DMN activation such as emotional processing, self-referential mental activity, and recollection of prior experiences (Raichle, 2015). However, microstate C has also been associated with regions of the saliency network (Britz et al., 2010) and there is recognition that further studies are required to better elucidate the underlying functional networks associated with microstate C (Michel & Koenig, 2018). Microstate D has been associated with the dorsal

attention network, which includes regions in the right superior and middle frontal gyri, as well as the right inferior and superior parietal lobules (Britz et al., 2010; Custo et al., 2017; Tarailis et al., 2023). Hence, while speculative, our finding of higher *occurrence* for microstate D in males compared to females might be interpreted as males in general more frequently engaging this network, and as also noted by Tomescu et al. (2018), males often outperform females on visuo-spatial processing tasks reliant on predominantly parietal brain regions (Gur et al., 2012; Seydell-Greenwald et al., 2017; Weiss et al., 2003). However, an important caveat here is that present study's findings were extracted from brain activity recorded at rest.

In contrast to these previous studies, we also found additional sex-related effects for microstates A and E. Specifically, females were shown to have greater values for all parameters for microstate A for the eyes-closed and eyes-open recordings, as well as for all parameters for the eyes-closed recordings for microstate E. The precise neurobiological mechanisms responsible for these sex-related differences remain unclear. However, while speculative, these might point to differential maturation of functional network architecture between males and females in keeping with findings from the broader literature (Gilmore et al., 2018; Sacher et al., 2013).

4.3 | Associations with alpha power

We found a positive association between all four microstate parameters and the aperiodic-adjusted alpha power for microstate C (eyes-closed and eyes-open recordings), as well as a negative association between alpha power and *GEV, coverage*, and *occurrence* for microstate E in the eyes-closed condition (Figure 7). We cautiously interpret this finding as indicating that the neural generators of microstate C show increased activation during periods of greater alpha power, in line with other authors (Croce et al., 2020), while, to a lesser extent, the generators of microstate E show reduced activation with higher alpha power. If microstate C does indeed represent a task-negative state, as suggested by research linking it to the DMN (Custo et al., 2017; Seitzman et al., 2017; Zappasodi et al., 2019), the positive association with alpha power appears rational, given links between alpha oscillations and cortical idling (Pfurtscheller et al., 1996) and DMN activation (Knyazev et al., 2011). Indeed, the underlying cortical sources of microstate C have been shown to overlap with key regions of the DMN (Custo et al., 2017). Research using simultaneous EEG-fMRI, has also demonstrated that visual alpha power is positively correlated with DMN BOLD activity (Mo et al., 2013), while a recent study by Clancy et al. (2022) showed that augmentation of alpha oscillations through non-invasive neuromodulation was able to strengthen connectivity of the DMN thus providing a compelling mechanistic association between alpha oscillations and DMN activity. This also appears to align with research showing increased prominence of microstates C and D during resting-state, compared to cognitive tasks, i.e., when the brain is disengaged from the sensory environment (Milz et al., 2016). However, further work is certainly required to clarify this association, as microstate C has also been linked to activation of the

saliency network (Britz et al., 2010). Similarly, while far less is currently known about the functional significance of microstate E, it is likely to also form part of the DMN (Brechet et al., 2019; Custo et al., 2017; Tarailis et al., 2023), yet here was negatively associated with alpha power.

Previous study has established oscillations within the alpha frequency band as a strong driver of microstate spatio-temporal dynamics. For example, using source-localised EEG data, Milz et al. (2017) reported that intracortical alpha oscillations primarily account for the various microstate classes. In line with our present results, a recent study conducted in adults by Croce et al. (2020) further found a positive association between alpha power and microstate C *duration*, while Antonova et al. (2022) also reported relative alpha power to be positively correlated with *duration* across the four canonical microstates (A–D; taken from EEG recorded during either mind wandering, or verbal/visual processing). Recently, Zulliger et al. (2022) also reported systematic alterations in local EEG spectral power that were associated with several microstate features (*duration*, *contribution*, and *occurrence*). In particular, it was noted that the spatial variance shared between time-varying microstate features and spectral power was particularly high in the alpha band for microstate class C (but shared spatial variance was also present between microstate class C and the theta and beta bands, as well as for other microstate classes).

Within a neurodevelopmental setting, our present findings also partially align with Takarae et al. (2022) who, using eyes-open resting-state EEG recordings form children and adolescents between seven and 19 years of age, found a positive association between microstate C *occurrence* and alpha power. However, these authors also found a negative association between microstate C duration and alpha power, which we did not observe in the present study. It is important to note, however, that here we calculated alpha power after first removing the aperiodic (i.e., non-oscillatory) broadband signal from the recording. As neural oscillations co-exist with aperiodic activity in the EEG signal, not accounting for their presence therefore risks conflating oscillatory and aperiodic components potentially leading to invalid or inaccurate interpretation of results (Donoghue et al., 2021; Donoghue, Dominguez, & Voytek, 2020). This is a particularly important consideration for neurodevelopmental cohorts where age-related changes in aperiodic activity can be strikingly apparent (Cellier et al., 2021; He et al., 2019; Hill et al., 2022). It is therefore possible that this methodological difference, along with other factors such as age, might have led to discrepancies between our present findings and previous observations. Exploring potential associations between various microstate spatio-temporal features and neuronal oscillations across different frequencies, after accounting for the aperiodic signal could be an interesting future research endeavour.

4.4 | Potential limitations and future directions

It is important to highlight some potential limitations of the present study. First, our microstate analyses were conducted on the broadband EEG signal (1–40 Hz), spanning a range of neural oscillatory frequencies (i.e., delta through low gamma). While this is a very common approach taken in contemporary microstate analysis it prevents examination of the specific influence of individual discrete frequency bands. It is possible that more fine-grained information might be able to be captured through the analysis of microstates across discrete narrow frequency bands (Ferat et al., 2022). Future study might therefore benefit from investigating spectrally specific microstate analyses in developmental cohorts. Second, given the limited research investigating EEG microstates in neurotypical children, our study was exploratory in nature and requires replication by additional studies, ideally using longitudinal designs and including additional microstates beyond the four canonical topographies (A–D). Finally, as we did not perform any source-localisation of the EEG signal, we cannot comment on specific cortical generators of the microstate classes. We chose not to perform source estimation as we did not have individual participant MRI scans, or high-resolution EEG recordings (i.e., >128 channels), which are typically required for accurate source reconstruction (Brodbeck et al., 2011; Song et al., 2015). Future study using high-density EEG and structural MRI scans for each participant might be valuable for further pinpointing specific cortical regions and networks underlying various microstate topographies.

4.5 | Conclusion

Since their establishment in the 1970's, there has been growing interest in the use of EEG-derived microstates as a means of understanding large-scale brain dynamics in both health and disease. Here, we have explored temporal features of five microstate classes (A–E) taken from both eyes-closed and eyes-open recordings and their associations with age, biological sex, and alpha oscillatory power in a large cohort of typically developing children. Our results provide important insight into functional brain dynamics during this critical neurodevelopmental period and significantly extend previous research conducted in adult populations. This provides an important framework for future research, which could extend these analyses to examine how various microstate parameters are disrupted in neurodevelopmental and neuropsychiatric disorders associated with alterations in large-scale brain network architecture such as autism, depression, and schizophrenia.

CONFLICT OF INTEREST STATEMENT

DATA AVAILABILITY STATEMENT

The data that support the findings of this study are available on reasonable request from the corresponding author. The data are not publicly available due to privacy or ethical restrictions.

REFERENCES

Agcaoglu, O., Wilson, T. W., Wang, Y. P., Stephen, J., & Calhoun, V. D. (2019). Resting state connectivity differences in eyes open versus eyes closed conditions. *Human Brain Mapping*, 40(8), 2488–2498. https://doi.org/10.1002/hbm.24539

Andreou, C., Faber, P. L., Leicht, G., Schoettle, D., Polomac, N., Hanganu-Opatz, I. L., Lehmann, D., & Mulert, C. (2014). Resting-state connectivity in the prodromal phase of schizophrenia: Insights from EEG microstates. *Schizophrenia Research*, 152(2–3), 513–520. https://doi.org/10.1016/j.schres.2013.12.008

Antonova, E., Holding, M., Suen, H. C., Sumich, A., Maex, R., & Nehaniv, C. (2022). EEG microstates: Functional significance and short-term test-retest reliability. *Neuroimage: Reports*, 2(2), 100089. https://doi.org/10.1016/j.ynirp.2022.100089

Bagdasarov, A., Roberts, K., Brechet, L., Brunet, D., Michel, C. M., & Gaffrey, M. S. (2022). Spatiotemporal dynamics of EEG microstates in four- to eight-year-old children: Age- and sex-related effects. *Developmental Cognitive Neuroscience*, 57, 101134. https://doi.org/10.1016/j.dcn.2022.101134

Bailey, N. W., Biabani, M., Hill, A. T., Miljevic, A., Rogasch, N. C., McQueen, B., Murphy, O. W., & Fitzgerald, P. B. (2023). Introducing RELAX: An automated pre-processing pipeline for cleaning EEG data—part 1: Algorithm and application to oscillations. *Clinical Neurophysiology*, 149, 178–201. https://doi.org/10.1016/j.clinph.2023.01.017

Bailey, N. W., Hill, A. T., Biabani, M., Murphy, O. W., Rogasch, N. C., McQueen, B., Miljevic, A., & Fitzgerald, P. B. (2023). RELAX part 2: A fully automated EEG data cleaning algorithm that is applicable to event-related-potentials. *Clinical Neurophysiology*, 149, 202–222. https://doi.org/10.1016/j.clinph.2023.01.018

Baldini, S., Morelli, M. E., Sartori, A., Pasquin, F., Dinoto, A., Bratina, A., Bosco, A., & Manganotti, P. (2023). Microstates in multiple sclerosis: An electrophysiological signature of altered large-scale networks functioning? *Brain Communication*, 5(1), fcac255. https://doi.org/10.1093/braincomms/fcac255

Betzel, R. F., Byrge, L., He, Y., Goni, J., Zuo, X. N., & Sporns, O. (2014). Changes in structural and functional connectivity among resting-state networks across the human lifespan. *NeuroImage*, 102, 345–357. https://doi.org/10.1016/j.neuroimage.2014.07.067

Bigdely-Shamlo, N., Mullen, T., Kothe, C., Su, K. M., & Robbins, K. A. (2015). The PREP pipeline: Standardized preprocessing for large-scale EEG analysis. *Frontiers in Neuroinformatics*, 9, 16. https://doi.org/10.3389/fninf.2015.00016

Bigelow, F. J., Clark, G. M., Lum, J. A. G., & Enticott, P. G. (2022). Facial emotion processing and language during early-to-middle childhood development: An event related potential study. *Developmental Cognitive Neuroscience*, 53, 101052. https://doi.org/10.1016/j.dcn.2021.101052

Bochet, A., Sperdin, H. F., Rihs, T. A., Kojovic, N., Franchini, M., Jan, R. K., Michel, C. M., & Schaer, M. (2021). Early alterations of large-scale brain networks temporal dynamics in young children with autism. *Communications Biology*, 4(1), 968. https://doi.org/10.1038/s42003-021-02494-3

Brechet, L., Brunet, D., Birot, G., Gruetter, R., Michel, C. M., & Jorge, J. (2019). Capturing the spatiotemporal dynamics of self-generated, task-initiated thoughts with EEG and fMRI. *NeuroImage*, 194, 82–92. https://doi.org/10.1016/j.neuroimage.2019.03.029

Britz, J., van de Ville, D., & Michel, C. M. (2010). BOLD correlates of EEG topography reveal rapid resting-state network dynamics. *NeuroImage*, 52(4), 1162–1170. https://doi.org/10.1016/j.neuroimage.2010.02.052

Brodbeck, V., Spinelli, L., Lascano, A. M., Wissmeier, M., Vargas, M. I., Vulliemoz, S., Pollo, C., Schaller, K., Michel, C. M., & Seeck, M. (2011). Electroencephalographic source imaging: A prospective study of 152 operated epileptic patients. *Brain*, 134(Pt 10), 2887–2897. https://doi.org/10.1093/brain/awr243

Buckner, R. L., Andrews-Hanna, J. R., & Schacter, D. L. (2008). The brain's default network: Anatomy, function, and relevance to disease. *Annals of the new York Academy of Sciences*, 1124, 1–38. https://doi.org/10.1196/annals.1440.011

Bunge, S. A., & Wright, S. B. (2007). Neurodevelopmental changes in working memory and cognitive control. *Current Opinion in Neurobiology*, 17(2), 243–250. https://doi.org/10.1016/j.conb.2007.02.005

Buzsáki, G., Anastassiou, C. A., & Koch, C. (2012). The origin of extracellular fields and currents: EEG, ECoG, LFP and spikes. *Nature Reviews Neuroscience*, 13(6), 407–420.

Casey, B. J., Galvan, A., & Hare, T. A. (2005). Changes in cerebral functional organization during cognitive development. *Current Opinion in Neurobiology*, 15(2), 239–244. https://doi.org/10.1016/j.conb.2005.03.012

Castellanos, N. P., & Makarov, V. A. (2006). Recovering EEG brain signals: Artifact suppression with wavelet enhanced independent component analysis. *Journal of Neuroscience Methods*, 158(2), 300–312. https://doi.org/10.1016/j.jneumeth.2006.05.033

Cellier, D., Riddle, J., Petersen, I., & Hwang, K. (2021). The development of theta and alpha neural oscillations from ages 3 to 24 years. *Developmental Cognitive Neuroscience*, 50, 100969. https://doi.org/10.1016/j.dcn.2021.100969

Chai, L. R., Khambhati, A. N., Ciric, R., Moore, T. M., Gur, R. C., Gur, R. E., Satterthwaite, T. D., & Bassett, D. S. (2017). Evolution of brain network dynamics in neurodevelopment. *Network Neuroscience*, 1(1), 14–30. https://doi.org/10.1162/NETN_a_00001

Clancy, K. J., Andrzejewski, J. A., You, Y., Rosenberg, J. T., Ding, M., & Li, W. (2022). Transcranial stimulation of alpha oscillations up-regulates the default mode network. *Proceedings of the National Academy of Sciences of the United States of America*, 119(1), e2110868119. https://doi.org/10.1073/pnas.2110868119

Cohen, M. X. (2017). Where does EEG come from and what does it mean? *Trends in Neurosciences*, 40(4), 208–218. https://doi.org/10.1016/j.tins.2017.02.004

Croce, P., Quercia, A., Costa, S., & Zappasodi, F. (2020). EEG microstates associated with intra- and inter-subject alpha variability. *Scientific Reports*, 10(1), 2469. https://doi.org/10.1038/s41598-020-58787-w

Custo, A., van de Ville, D., Wells, W. M., Tomescu, M. I., Brunet, D., & Michel, C. M. (2017). Electroencephalographic resting-state networks: Source localization of microstates. *Brain Connectivity*, 7(10), 671–682. https://doi.org/10.1089/brain.2016.0476

D'Croz-Baron, D. F., Baker, M., Michel, C. M., & Karp, T. (2019). EEG microstates analysis in young adults with autism Spectrum disorder during resting-state. *Frontiers in Human Neuroscience*, 13, 173. https://doi.org/10.3389/fnhum.2019.00173

da Cruz, J. R., Favrod, O., Roinishvili, M., Chkonia, E., Brand, A., Mohr, C., Figueiredo, P., & Herzog, M. H. (2020). EEG microstates are a candidate endophenotype for schizophrenia. *Nature Communications*, 11(1), 3089. https://doi.org/10.1038/s41467-020-16914-1

Das, S., Zomorrodi, R., Enticott, P. G., Kirkovski, M., Blumberger, D. M., Rajji, T. K., & Desarkar, P. (2022). Resting state electroencephalography microstates in autism spectrum disorder: A mini-review. *Frontiers in Psychiatry*, 13, 988939. https://doi.org/10.3389/fpsyt.2022.988939

Delorme, A., & Makeig, S. (2004). EEGLAB: An open source toolbox for analysis of single-trial EEG dynamics including independent component analysis. *Journal of Neuroscience Methods*, 134(1), 9–21.

Donoghue, T., Dominguez, J., & Voytek, B. (2020). Electrophysiological frequency band ratio measures conflate periodic and aperiodic neural activity. *eNeuro*, 7(6). https://doi.org/10.1523/ENEURO.0192-20.2020

Donoghue, T., Haller, M., Peterson, E. J., Varma, P., Sebastian, P., Gao, R., Noto, T., Lara, A. H., Wallis, J. D., Knight, R. T., Shestyuk, A., &

Voytek, B. (2020). Parameterizing neural power spectra into periodic and aperiodic components. *Nature Neuroscience*, *23*(12), 1655–1665. https://doi.org/10.1038/s41593-020-00744-x

Donoghue, T., Schaworonkow, N., & Voytek, B. (2021). Methodological considerations for studying neural oscillations. *The European Journal of Neuroscience*, *55*, 3502–3527. https://doi.org/10.1111/ejn.15361

Ekstrom, A. (2010). How and when the fMRI BOLD signal relates to underlying neural activity: The danger in dissociation. *Brain Research Reviews*, *62*(2), 233–244. https://doi.org/10.1016/j.brainresrev.2009.12.004

Fair, D. A., Cohen, A. L., Power, J. D., Dosenbach, N. U., Church, J. A., Miezin, F. M., Schlaggar, B. L., & Petersen, S. E. (2009). Functional brain networks develop from a "local to distributed" organization. *PLoS Computational Biology*, *5*(5), e1000381. https://doi.org/10.1371/journal.pcbi.1000381

Fan, F., Liao, X., Lei, T., Zhao, T., Xia, M., Men, W., Wang, Y., Hu, M., Liu, J., Qin, S., Tan, S., Gao, J. H., Dong, Q., Tao, S., & He, Y. (2021). Development of the default-mode network during childhood and adolescence: A longitudinal resting-state fMRI study. *NeuroImage*, *226*, 117581. https://doi.org/10.1016/j.neuroimage.2020.117581

Faul, F., Erdfelder, E., Lang, A. G., & Buchner, A. (2007). G*Power 3: A flexible statistical power analysis program for the social, behavioral, and biomedical sciences. *Behavior Research Methods*, *39*(2), 175–191.

Ferat, V., Seeber, M., Michel, C. M., & Ros, T. (2022). Beyond broadband: Towards a spectral decomposition of electroencephalography microstates. *Human Brain Mapping*, *43*(10), 3047–3061. https://doi.org/10.1002/hbm.25834

Gilmore, J. H., Knickmeyer, R. C., & Gao, W. (2018). Imaging structural and functional brain development in early childhood. *Nature Reviews. Neuroscience*, *19*(3), 123–137. https://doi.org/10.1038/nrn.2018.1

Gu, S., Satterthwaite, T. D., Medaglia, J. D., Yang, M., Gur, R. E., Gur, R. C., & Bassett, D. S. (2015). Emergence of system roles in normative neurodevelopment. *Proceedings of the National Academy of Sciences of the United States of America*, *112*(44), 13681–13686. https://doi.org/10.1073/pnas.1502829112

Gur, R. C., Richard, J., Calkins, M. E., Chiavacci, R., Hansen, J. A., Bilker, W. B., Loughead, J., Connolly, J. J., Qiu, H., Mentch, F. D., Abou-Sleiman, P. M., Hakonarson, H., & Gur, R. E. (2012). Age group and sex differences in performance on a computerized neurocognitive battery in children age 8-21. *Neuropsychology*, *26*(2), 251–265. https://doi.org/10.1037/a0026712

Hampson, M., Driesen, N. R., Skudlarski, P., Gore, J. C., & Constable, R. T. (2006). Brain connectivity related to working memory performance. *The Journal of Neuroscience*, *26*(51), 13338–13343. https://doi.org/10.1523/JNEUROSCI.3408-06.2006

He, B. J. (2014). Scale-free brain activity: Past, present, and future. *Trends in Cognitive Sciences*, *18*(9), 480–487. https://doi.org/10.1016/j.tics.2014.04.003

He, W., Donoghue, T., Sowman, P. F., Seymour, R. A., Brock, J., Crain, S., Voytek, B., & Hillebrand, A. (2019). Co-increasing neuronal noise and beta power in the developing brain. *bioRxiv*, 839258. https://doi.org/10.1101/839258

Hill, A. T., Clark, G. M., Bigelow, F. J., Lum, J. A. G., & Enticott, P. G. (2022). Periodic and aperiodic neural activity displays age-dependent changes across early-to-middle childhood. *Developmental Cognitive Neuroscience*, *54*, 101076. https://doi.org/10.1016/j.dcn.2022.101076

Holm, S. (1979). A simple sequentially rejective multiple test procedure. *Scandinavian Journal of Statistics*, *6*(2), 65–70.

Huang, H., Shu, N., Mishra, V., Jeon, T., Chalak, L., Wang, Z. J., Rollins, N., Gong, G., Cheng, H., Peng, Y., Dong, Q., & He, Y. (2015). Development of human brain structural networks through infancy and childhood. *Cerebral Cortex*, *25*(5), 1389–1404. https://doi.org/10.1093/cercor/bht335

John, E., Ahn, H., Prichep, L., Trepetin, M., Brown, D., & Kaye, H. (1980). Developmental equations for the electroencephalogram. *Science*, *210*(4475), 1255–1258. https://doi.org/10.1126/science.7434026

Ke, M., Li, J., & Wang, L. (2021). Alteration in resting-state EEG microstates following 24 hours of Total sleep deprivation in healthy young male subjects. *Frontiers in Human Neuroscience*, *15*, 636252. https://doi.org/10.3389/fnhum.2021.636252

Khanna, A., Pascual-Leone, A., & Farzan, F. (2014). Reliability of resting-state microstate features in electroencephalography. *PLoS One*, *9*(12), e114163. https://doi.org/10.1371/journal.pone.0114163

Khanna, A., Pascual-Leone, A., Michel, C. M., & Farzan, F. (2015). Microstates in resting-state EEG: Current status and future directions. *Neuroscience and Biobehavioral Reviews*, *49*, 105–113. https://doi.org/10.1016/j.neubiorev.2014.12.010

Klimesch, W., Schack, B., & Sauseng, P. (2005). The functional significance of theta and upper alpha oscillations. *Experimental Psychology*, *52*(2), 99–108. https://doi.org/10.1027/1618-3169.52.2.99

Knyazev, G. G., Slobodskoj-Plusnin, J. Y., Bocharov, A. V., & Pylkova, L. V. (2011). The default mode network and EEG alpha oscillations: An independent component analysis. *Brain Research*, *1402*, 67–79. https://doi.org/10.1016/j.brainres.2011.05.052

Koenig, T., Prichep, L., Lehmann, D., Sosa, P. V., Braeker, E., Kleinlogel, H., Isenhart, R., & John, E. R. (2002). Millisecond by millisecond, year by year: Normative EEG microstates and developmental stages. *NeuroImage*, *16*(1), 41–48. https://doi.org/10.1006/nimg.2002.1070

Lehmann, D., & Skrandies, W. (1980). Reference-free identification of components of checkerboard-evoked multichannel potential fields. *Electroencephalography and Clinical Neurophysiology*, *48*(6), 609–621. https://doi.org/10.1016/0013-4694(80)90419-8

Lehmann, D., Ozaki, H., & Pal, I. (1987). EEG alpha map series: Brain microstates by space-oriented adaptive segmentation. *Electroencephalography and Clinical Neurophysiology*, *67*(3), 271–288. https://doi.org/10.1016/0013-4694(87)90025-3

Li, L. (2010). The differences among eyes-closed, eyes-open and attention states: An EEG study. Paper presented at the 2010 6th International Conference on Wireless Communications Networking and Mobile Computing (WiCOM), 23–25 September 2010.

Long, X., Benischek, A., Dewey, D., & Lebel, C. (2017). Age-related functional brain changes in young children. *NeuroImage*, *155*, 322–330. https://doi.org/10.1016/j.neuroimage.2017.04.059

Michel, C. M., & Koenig, T. (2018). EEG microstates as a tool for studying the temporal dynamics of whole-brain neuronal networks: A review. *NeuroImage*, *180*, 577–593. https://doi.org/10.1016/j.neuroimage.2017.11.062

Milz, P., Faber, P. L., Lehmann, D., Koenig, T., Kochi, K., & Pascual-Marqui, R. D. (2016). The functional significance of EEG microstates: Associations with modalities of thinking. *NeuroImage*, *125*, 643–656. https://doi.org/10.1016/j.neuroimage.2015.08.023

Milz, P., Pascual-Marqui, R. D., Achermann, P., Kochi, K., & Faber, P. L. (2017). The EEG microstate topography is predominantly determined by intracortical sources in the alpha band. *NeuroImage*, *162*, 353–361. https://doi.org/10.1016/j.neuroimage.2017.08.058

Mo, J., Liu, Y., Huang, H., & Ding, M. (2013). Coupling between visual alpha oscillations and default mode activity. *NeuroImage*, *68*, 112–118. https://doi.org/10.1016/j.neuroimage.2012.11.058

Musaeus, C. S., Nielsen, M. S., & Hogh, P. (2019). Microstates as disease and progression markers in patients with mild cognitive impairment. *Frontiers in Neuroscience*, *13*, 563. https://doi.org/10.3389/fnins.2019.00563

Musso, F., Brinkmeyer, J., Mobascher, A., Warbrick, T., & Winterer, G. (2010). Spontaneous brain activity and EEG microstates. A novel EEG/fMRI analysis approach to explore resting-state networks. *NeuroImage*, *52*(4), 1149–1161. https://doi.org/10.1016/j.neuroimage.2010.01.093

Niedermeyer, E. (1999). The normal EEG of the waking adult. In E. Niedermeyer & F. Lopes da Silva (Eds.), *Electroencephalography: Basic principles, clinical applications, and related fields* (5th ed., pp. 167–192). Lippincott Williams & Wilkins.

Olejniczak, P. (2006). Neurophysiologic basis of EEG. *Journal of Clinical Neurophysiology*, *23*(3), 186–189. https://doi.org/10.1097/01.wnp.0000220079.61973.6c

Ostlund, B., Donoghue, T., Anaya, B., Gunther, K. E., Karalunas, S. L., Voytek, B., & Perez-Edgar, K. E. (2022). Spectral parameterization for studying neurodevelopment: How and why. *Developmental Cognitive Neuroscience*, *54*, 101073. https://doi.org/10.1016/j.dcn.2022.101073

Padmanabhan, A., Lynch, C. J., Schaer, M., & Menon, V. (2017). The default mode network in autism. *Biological Psychiatry: Cognitive Neuroscience and Neuroimaging*, *2*(6), 476–486. https://doi.org/10.1016/j.bpsc.2017.04.004

Pascual-Marqui, R. D., Michel, C. M., & Lehmann, D. (1995). Segmentation of brain electrical activity into microstates: Model estimation and validation. *IEEE Transactions on Biomedical Engineering*, *42*(7), 658–665. https://doi.org/10.1109/10.391164

Pfurtscheller, G., Stancák, A., & Neuper, C. (1996). Event-related synchronization (ERS) in the alpha band: An electrophysiological correlate of cortical idling—A review. *International Journal of Psychophysiology*, *24*(1), 39–46. https://doi.org/10.1016/S0167-8760(96)00066-9

Pion-Tonachini, L., Kreutz-Delgado, K., & Makeig, S. (2019). ICLabel: An automated electroencephalographic independent component classifier, dataset, and website. *NeuroImage*, *198*, 181–197. https://doi.org/10.1016/j.neuroimage.2019.05.026

Poulsen, A. T., Pedroni, A., Langer, N., & Hansen, L. K. (2018). Microstate EEGlab toolbox: An introductory guide. *bioRxiv*, 289850. https://doi.org/10.1101/289850

Power, J. D., Fair, D. A., Schlaggar, B. L., & Petersen, S. E. (2010). The development of human functional brain networks. *Neuron*, *67*(5), 735–748. https://doi.org/10.1016/j.neuron.2010.08.017

R Core Team. (2020). *R: A language environment for statistical computing*. R Foundation for Statistical Computing.

Raichle, M. E. (2015). The brain's default mode network. *Annual Review of Neuroscience*, *38*, 433–447. https://doi.org/10.1146/annurev-neuro-071013-014030

Sacher, J., Neumann, J., Okon-Singer, H., Gotowiec, S., & Villringer, A. (2013). Sexual dimorphism in the human brain: Evidence from neuroimaging. *Magnetic Resonance Imaging*, *31*(3), 366–375. https://doi.org/10.1016/j.mri.2012.06.007

Seitzman, B. A., Abell, M., Bartley, S. C., Erickson, M. A., Bolbecker, A. R., & Hetrick, W. P. (2017). Cognitive manipulation of brain electric microstates. *NeuroImage*, *146*, 533–543. https://doi.org/10.1016/j.neuroimage.2016.10.002

Seydell-Greenwald, A., Ferrara, K., Chambers, C. E., Newport, E. L., & Landau, B. (2017). Bilateral parietal activations for complex visual-spatial functions: Evidence from a visual-spatial construction task. *Neuropsychologia*, *106*, 194–206. https://doi.org/10.1016/j.neuropsychologia.2017.10.005

Sherman, L. E., Rudie, J. D., Pfeifer, J. H., Masten, C. L., McNealy, K., & Dapretto, M. (2014). Development of the default mode and central executive networks across early adolescence: A longitudinal study. *Developmental Cognitive Neuroscience*, *10*, 148–159. https://doi.org/10.1016/j.dcn.2014.08.002

Singh, K. D. (2012). Which "neural activity" do you mean? fMRI, MEG, oscillations and neurotransmitters. *NeuroImage*, *62*(2), 1121–1130. https://doi.org/10.1016/j.neuroimage.2012.01.028

Smallwood, J., Bernhardt, B. C., Leech, R., Bzdok, D., Jefferies, E., & Margulies, D. S. (2021). The default mode network in cognition: A topographical perspective. *Nature Reviews. Neuroscience*, *22*, 503–513. https://doi.org/10.1038/s41583-021-00474-4

Somers, B., Francart, T., & Bertrand, A. (2018). A generic EEG artifact removal algorithm based on the multi-channel wiener filter. *Journal of Neural Engineering*, *15*(3), 036007. https://doi.org/10.1088/1741-2552/aaac92

Song, J., Davey, C., Poulsen, C., Luu, P., Turovets, S., Anderson, E., Li, K., & Tucker, D. (2015). EEG source localization: Sensor density and head surface coverage. *Journal of Neuroscience Methods*, *256*, 9–21. https://doi.org/10.1016/j.jneumeth.2015.08.015

Supekar, K., Musen, M., & Menon, V. (2009). Development of large-scale functional brain networks in children. *PLoS Biology*, *7*(7), e1000157. https://doi.org/10.1371/journal.pbio.1000157

Takarae, Y., Zanesco, A., Keehn, B., Chukoskie, L., Muller, R. A., & Townsend, J. (2022). EEG microstates suggest atypical resting-state network activity in high-functioning children and adolescents with autism spectrum development. *Developmental Science*, *25*, e13231. https://doi.org/10.1111/desc.13231

Tarailis, P., Koenig, T., Michel, C. M., & Griskova-Bulanova, I. (2023). The functional aspects of resting EEG microstates: A systematic review. *Brain Topography*. https://doi.org/10.1007/s10548-023-00958-9

Tarailis, P., Šimkutė, D., Koenig, T., & Griškova-Bulanova, I. (2021). Relationship between spatiotemporal dynamics of the brain at rest and self-reported spontaneous thoughts: An EEG microstate approach. *Journal of Personalized Medicine*, *11*(11), 1216. https://doi.org/10.3390/jpm11111216

Tomescu, M. I., Rihs, T. A., Rochas, V., Hardmeier, M., Britz, J., Allali, G., Fuhr, P., Eliez, S., & Michel, C. M. (2018). From swing to cane: Sex differences of EEG resting-state temporal patterns during maturation and aging. *Developmental Cognitive Neuroscience*, *31*, 58–66. https://doi.org/10.1016/j.dcn.2018.04.011

Uhlhaas, P. J., Roux, F., Rodriguez, E., Rotarska-Jagiela, A., & Singer, W. (2010). Neural synchrony and the development of cortical networks. *Trends in Cognitive Sciences*, *14*(2), 72–80. https://doi.org/10.1016/j.tics.2009.12.002

Vogel, A. C., Power, J. D., Petersen, S. E., & Schlaggar, B. L. (2010). Development of the brain's functional network architecture. *Neuropsychology Review*, *20*(4), 362–375. https://doi.org/10.1007/s11065-010-9145-7

Wang, J., Barstein, J., Ethridge, L. E., Mosconi, M. W., Takarae, Y., & Sweeney, J. A. (2013). Resting state EEG abnormalities in autism spectrum disorders. *Journal of Neurodevelopmental Disorders*, *5*(1), 24. https://doi.org/10.1186/1866-1955-5-24

Weiss, E. M., Kemmler, G., Deisenhammer, E. A., Fleischhacker, W. W., & Delazer, M. (2003). Sex differences in cognitive functions. *Personality and Individual Differences*, *35*(4), 863–875. https://doi.org/10.1016/S0191-8869(02)00288-X

Zanesco, A. P., King, B. G., Skwara, A. C., & Saron, C. D. (2020). Within and between-person correlates of the temporal dynamics of resting EEG microstates. *NeuroImage*, *211*, 116631. https://doi.org/10.1016/j.neuroimage.2020.116631

Zappasodi, F., Perrucci, M. G., Saggino, A., Croce, P., Mercuri, P., Romanelli, R., Colom, R., & Ebisch, S. J. H. (2019). EEG microstates distinguish between cognitive components of fluid reasoning. *NeuroImage*, *189*, 560–573. https://doi.org/10.1016/j.neuroimage.2019.01.067

Zulliger, J., Diaz Hernandez, L., & Koenig, T. (2022). Within and between subject spectral fingerprints of EEG-microstate parameters. *Brain Topography*, *35*(3), 277–281. https://doi.org/10.1007/s10548-022-00896-y

SUPPORTING INFORMATION

Additional supporting information can be found online in the Supporting Information section at the end of this article.